J|A|C|S
ARTICLES
Published on Web 05/04/2007

Chiral Brønsted Acid Catalyzed Enantioselective Mannich-Type Reaction

Masahiro Yamanaka,*,‡ Junji Itoh,† Kohei Fuchibe,† and Takahiko Akiyama*,†

Contribution from the Department of Chemistry, Faculty of Science, Gakushuin University, 1-5-1 Mejiro Toshima-ku, Tokyo 171-8588, Japan, and Department of Chemistry, Faculty of Science, Rikkyo University, 3-34-1 Nishi-Ikebukuro, Toshima-ku, Tokyo 171-8501 Japan

Received November 27, 2006; E-mail: takahiko.akiyama@gakushuin.ac.jp; myamanaka@rikkyo.ac.jp

Abstract: Mannich-type reaction of ketene silyl acetals with aldimines proceeded catalytically by means of a phosphoric acid diester, derived from (*R*)-BINOL, as a chiral Brønsted acid to afford β-amino esters with good diastereoselectivity in favor of the *syn* isomer and high enantioselectivity (up to 96% ee). The highest enantioselectivity was achieved by the phosphoric acid diester bearing 4-nitrophenyl groups on the 3,3′-positions of BINOL. The *N*-2-hydroxyphenyl group of aldimine was found to be essential for the present Mannich-type reaction. In combination with these experimental investigations, two possible monocoordination and dicoordination pathways were explored using density functional theory calculations (BHandHLYP/6-31G*). The present reaction proceeds via a dicoordination pathway through the zwitterionic and nine-membered cyclic transition state (TS) consisting of the aldimine and the phosphoric acid. The *re*-facial selectivity was also well-rationalized theoretically. The nine-membered cyclic structure and aromatic stacking interaction between the 4-nitrophenyl group and *N*-aryl group would fix the geometry of aldimine on the transition state, and the *si*-facial attacking TS is less favored by the steric hindrance of the 3,3′-aryl substituents.

Introduction

Development of efficient chiral catalysts continues to be one of the most challenging topics in organic chemistry.[1] A number of metal-based Lewis acid catalysts have been developed for the activation of a carbon−oxygen double bond as well as a carbon−nitrogen double bond, and highly enantioselective carbon−carbon bond formation reactions have been realized. In contrast to metal-based Lewis acids, organocatalysts are generally stable toward water and oxygen, hence being easy to handle. As pioneering works of this area by Jacobsen[2] and Takemoto,[3] chiral thiourea derivatives have been recognized as efficient catalysts for the nucleophilic addition reaction toward aldehydes and aldimines. Furthermore, TADDOL has been found to be quite effective as a chiral catalyst for the cycloaddition reaction toward aldehyde.[4] These asymmetric organocatalysis should be classified as hydrogen-bonding catalysis. On the other hand, a Brønsted acid acts as a stronger electrophilic activator (e.g., protonation) than a neutral organic molecule in hydrogen-bonding catalysis (Figure 1). In spite of being a stronger and valuable electrophilic activator, Brønsted acids had been scarcely employed for catalytic asymmetric reactions when our project of chiral Brønsted acid catalysis was started.[5−7] Until quite recently, chiral Brønsted acid catalysis[8] had been an underdeveloped area except for asymmetric protonation reactions.[9] Therefore, a chiral Brønsted acid catalyst will be a new

† Gakushuin University.
‡ Rikkyo University.

(1) Jacobsen, E., Pfaltz, A., Yamamoto, H., Eds. *Comprehensive Asymmetric Catalysis*, Vols. I, II, III; Springer-Verlag: Berlin, 1999. Tye, H.; Comina, P. J. *J. Chem. Soc., Perkin Trans. 1* **2001**, 1729−1747.

(2) (a) Sigman, M. S.; Vachal, P.; Jacobsen, E. N. *Angew. Chem., Int. Ed.* **2000**, *39*, 1279−1281. (b) Wenzel, A. G.; Jacobsen, E. N. *J. Am. Chem. Soc.* **2002**, *124*, 12964−12965. (c) Joly, G. D.; Jacobsen, E. N. *J. Am. Chem. Soc*. **2004**, *126*, 4102−4103. (d) Taylor, M. S.; Jacobsen, E. N. *J. Am. Chem. Soc.* **2004**, *126*, 10558−10559. (e) Fuerst, D. E.; Jacobsen, E. N. *J. Am. Chem. Soc.* **2005**, *127*, 8964−8965. (f) Taylor, M. S.; Tokunaga, N.; Jacobsen, E. N. *Angew. Chem., Int. Ed.* **2005**, *44*, 6700−6704. (g) Yoon, T. P.; Jacobsen, E. N. *Angew. Chem., Int. Ed.* **2005**, *44*, 466−468. (h) Taylor, M. S.; Jacobsen, E. N. *Angew. Chem., Int. Ed.* **2006**, *45*, 1520−1543. (i) Lalonde, M. P.; Chen, Y.; Jacobsen, E. N. *Angew. Chem., Int. Ed.* **2006**, *45*, 6366−6370.

(3) (a) Okino, T.; Hoashi, Y.; Takemoto, Y. *J. Am. Chem. Soc*. **2003**, *125*, 12672−12673. (b) Okino, T.; Hoashi, Y.; Takemoto, Y. *Tetrahedron Lett.* **2003**, *44*, 2817−2821. (c) Hoashi, Y.; Yabuta, T.; Takemoto, Y. *Tetrahedron Lett.* **2004**, *45*, 9185−9188. (d) Okino, T.; Nakamura, S.; Furukawa, T.; Takemoto, Y. *Org. Lett.* **2004**, *6*, 625−627. (e) Hoashi, Y.; Okino, T.; Takemoto, Y. *Angew. Chem., Int. Ed.* **2005**, *44*, 4032−4035. (f) Okino, T.; Hoashi, Y.; Furukawa, T.; Xu, X.; Takemoto, Y. *J. Am. Chem. Soc.* **2005**, *127*, 119−125. (g) Takemoto, Y. *Org. Biomol. Chem.* **2005**, *3*, 4299−4306. (h) Hoashi, Y.; Yabuta, T.; Yuan, P.; Miyabe, H.; Takemoto, Y. *Tetrahedron* **2006**, *62*, 365−374. (i) Inokuma, T.; Hoashi, Y.; Takemoto, Y. *J. Am. Chem. Soc.* **2006**, *128*, 9413−9419. (j) Xu, X.; Furukawa, T.; Okino, T.; Miyabe, H.; Takemoto, Y. *Chem.−Eur. J.* **2006**, *12*, 466−476.

(4) (a) Huang, Y.; Unni, A. K.; Thadani, A. N.; Rawal, V. H. *Nature* **2003**, *424*, 146. (b) Thadani, A. N.; Stankovic, A. R.; Rawal, V. H. *Proc. Natl. Acad. Sci. U.S.A.* **2004**, *101*, 5846−5850. (c) Unni, A. K.; Takenaka, N.; Yamamoto, H.; Rawal, V. H. *J. Am. Chem. Soc.* **2005**, *127*, 1336−1337. (d) Gondi, V. B.; Gravel, M.; Rawal, V. H. *Org. Lett.* **2005**, *7*, 5657−5660. (e) McGilvra, J. D.; Unni, A. K.; Modi, K.; Rawal, V. H. *Angew. Chem., Int. Ed.* **2006**, *45*, 6130−6133. (f) Du, H.; Zhao, D.; Ding, K. *Chem.−Eur. J.* **2004**, *10*, 5964−5970.

(5) For a preliminary communication, see; Akiyama, T.; Itoh, J.; Yokota, K.; Fuchibe, K. *Angew. Chem., Int. Ed.* **2004**, *43*, 1566−1568.

(6) Our report: (a) Akiyama, T.; Morita, H.; Itoh, J.; Fuchibe, K. *Org. Lett.* **2005**, *7*, 2583−2585. (b) Akiyama, T.; Saitoh, Y.; Morita, H.; Fuchibe, K. *Adv. Synth. Catal.* **2005**, *347*, 1523−1526. (c) Akiyama, T.; Tamura, Y.; Itoh, J.; Morita, H.; Fuchibe, K. *Synlett* **2006**, 141−143. (d) Itoh, J.; Fuchibe, K.; Akiyama, T. *Angew. Chem., Int. Ed.* **2006**, *45*, 4796−4798. (e) Akiyama, T.; Morita, H.; Fuchibe, K. *J. Am Chem. Soc*. **2006**, *128*, 13070−13071.

 10.1021/ja0684803 CCC: $37.00

Figure 1. Mode of activation by the acid catalysis.

entry to the metal-free organocatalysts as a rapidly emerging area in the fields of synthetic organic chemistry.[10]

A Mannich-type reaction of silyl enolate with aldimine is a useful method for the preparation of β-amino carbonyl compounds, which are the precursors of β-amino acids and β-lactams.[11] Various chiral Lewis acids have been developed as the catalyst for the Mannich-type reaction.[12−14] Focusing on the Mannich-type reaction as a model reaction, we have designed and synthesized stronger chiral Brønsted acid catalysts, which can be employed under an operationally simple procedure. A chiral cyclic phosphoric acid diester has been found to be quite effective as a chiral Brønsted acid; a Mannich-type reaction of silyl enolate with aldimine proceeded smoothly to give β-amino esters in good yields with good to excellent enantioselectivities. We describe herein the design of the chiral Brønsted acid catalyst and its application to the enantioselective Mannich-type reaction. A quantum chemical study was carried out to elucidate the reaction mechanism as well as the origin of the enantioselectivity.

Design of the Chiral Brønsted Acid Catalyst. Our preliminary investigation to develop a chiral Brønsted acid catalyst has revealed that HBF_4 and TsOH are effective for the activation of aldimines. The Mannich-type reaction of silyl enolate with aldimines proceeded smoothly under the influence of 10 mol % of HBF_4 in aqueous MeOH or THF to afford β-amino carbonyl compounds in good yields.[15] The same reaction can be achieved even in water in the coexistence of SDS (sodium dodecyl sulfate) as a surfactant (Scheme 1).[16] In addition, aza Diels−Alder reaction of aldimines with Danishefsky's diene under the same reaction conditions afforded six-membered heterocycles in good yields.[17]

Scheme 1. HBF_4-Catalyzed Mannich-Type Reaction and Aza Diels−Alder Reaction

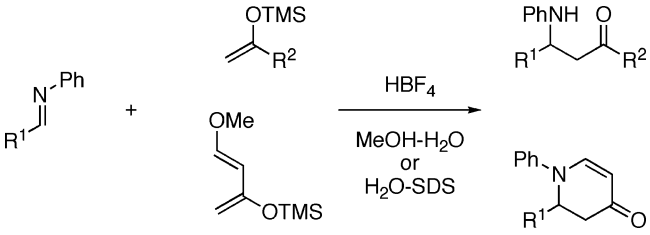

These findings drove us to challenge the development of the chiral Brønsted acid catalyst. A novel and useful chiral Brønsted acid was designed in view of the following three points.

(1) use of readily available chiral source: (*R*)-BINOL was selected as a chiral source.

(2) suitable acid strength for the reaction to proceed: phosphate is a candidate because the pK_a of $(EtO)_2P(O)OH$ is 1.3,[18] which is close to that of HBF_4 (−0.44).[19]

(3) cyclic structure for attaining high asymmetric induction: a cyclic phosphoric acid diester **1**, bearing BINOL scaffold, was selected as a chiral Brønsted acid.

(7) Reports by others: (a) Uraguchi, D.; Terada, M. *J. Am. Chem. Soc.* **2004**, *126*, 5356−5357. (b) Uraguchi, D.; Sorimachi, K.; Terada, M. *J. Am. Chem. Soc.* **2004**, *126*, 11804−11805. (c) Uraguchi, D.; Sorimachi, K.; Terada, M. *J. Am. Chem. Soc.* **2005**, *127*, 9360−9361. (d) Rueping, M.; Sugiono, E.; Azap, C.; Theissmann, T.; Bolte, M. *Org. Lett.* **2005**, *7*, 3781−3783. (e) Rowland, G. B.; Zhang, H.; Rowland, E. B.; Chennamadhavuni, S.; Wang, Y.; Antilla, J. C. *J. Am. Chem. Soc.* **2005**, *127*, 15696−15697. (f) Hoffmann, S.; Seayad, A. M.; List, B. *Angew. Chem., Int. Ed.* **2005**, *44*, 7424−7427. (g) Seayad, J.; Seayad, A. M.; List, B. *J. Am. Chem. Soc.* **2006**, *128*, 1086−1087. (h) Storer, R. I.; Carrera, D. E.; Ni, Y.; MacMillan, D. W. C. *J. Am. Chem. Soc.* **2006**, *128*, 84−86. (i) Terada, M.; Machioka, K.; Sorimachi, K. *Angew. Chem., Int. Ed.* **2006**, *45*, 2254−2257. (j) Rueping, M.; Sugiono, E.; Azap, C. *Angew. Chem., Int. Ed.* **2006**, *45*, 2617−2619. (k) Rueping, M.; Antonchick, A. P.; Theissmann, T. *Angew. Chem., Int. Ed.* **2006**, *45*, 3683−3686. (l) Nakashima, D.; Yamamoto, H. *J. Am. Chem. Soc.* **2006**, *128*, 9626−9627. (m) Hoffmann, S.; Nicoletti, M.; List, B. *J. Am Chem. Soc.* **2006**, *128*, 13074−13075. (n) Rueping, M.; Antonchick, A. P.; Theissmann, T. *Angew. Chem., Int. Ed.* **2006**, *45*, 6751−6755. (o) Chen, X.-H.; Xu, X.-Y.; Liu, H.; Cun, L.-F.; Gong, L.-Z. *J. Am. Chem. Soc.* **2006**, *128*, 14802−14803. (p) Rueping, M.; Azap, C. *Angew. Chem., Int. Ed.* **2006**, *45*, 7832−7835.
(8) For reviews on Brønsted acid catalysis, see: (a) Schreiner, P. R. *Chem. Soc. Rev.* **2003**, *32*, 289−296. (b) Pihko, P. M. *Angew. Chem., Int. Ed.* **2004**, *43*, 2062−2064. (c) Bolm, C.; Rantanen, T.; Schiffers, I.; Zani, L. *Angew. Chem., Int. Ed.* **2005**, *44*, 1758−1763. (d) Pihko, P. M. *Lett. Org. Chem.* **2005**, *2*, 398−403. (e) Takemoto, Y. *Org. Biomol. Chem.* **2005**, *3*, 4299−4306. (f) Taylor, M. S.; Jacobsen, E. N. *Angew. Chem., Int. Ed.* **2006**, *45*, 1520−1543. (g) Akiyama, T.; Itoh, J.; Fuchibe, K. *Adv. Synth. Catal.* **2006**, *348*, 999−1010. (h) Connon, S. J. *Angew. Chem., Int. Ed.* **2006**, *45*, 3909−3912.
(9) For a review, see: Yanagisawa, A.; Yamamoto, H. In *Comprehensive Asymmetric Catalysis*; Jacobsen, E. N.; Pfaltz, A.; Yamamoto, H., Eds.; Springer: New York, 1999; Chapter 34.2.
(10) (a) Dalko, P. I.; Moisan, L. *Angew. Chem., Int. Ed.* **2001**, *40*, 3726−3748. (b) Dalko, P. I.; Moisan, L. *Angew. Chem., Int. Ed.* **2004**, *43*, 5138−5175. Houk, K. N., List, B., Eds. (special issue on organocatalysis) *Acc. Chem. Res.* **2004**, *37*, 487−631. (d) List, B., Bolm, C., Eds. (special issue on organocatalysis) *Adv. Synth. Catal.* **2004**, *346*, 1021−1249. (e) Berkessel, A., Gröger, H., Eds. *Asymmetric Organocatalysis*, Wiley-VCH: Weinheim, 2005. (f) Seayad, J.; List, B. *Org. Biomol. Chem.* **2005**, *3*, 719−724.
(11) For reviews, see: Kleinman, E. F. In *Comprehensive Organic Synthesis, Vol. 2*; Trost, B. M., Fleming, I., Eds.; Pergamon Press: Oxford, 1991; p 893. Arend, M.; Westermann, B.; Risch, N. *Angew. Chem., Int. Ed.* **1998**, *37*, 1044−1070. Kobayashi, S.; Ishitani, H. *Chem. Rev.* **1999**, *99*, 1069−1094. Arend, M. *Angew. Chem., Int. Ed.* **1999**, *38*, 2873−2874.
(12) For selected examples of the enantioselective Mannich-type reaction by means of stoichiometric amount of activator, see: (a) Ishihara, K.; Miyata, M.; Hattori, K.; Tada, T.; Yamamoto, H. *J. Am. Chem. Soc.* **1994**, *116*, 10520−10524. (b) Müller, R.; Goesmann, H.; Waldmann, H. *Angew. Chem., Int. Ed.* **1999**, *38*, 184−187.
(13) For selected examples of the chiral Lewis acid catalyzed reactions, see: (a) Ishitani, H.; Ueno, M.; Kobayashi, S. *J. Am. Chem. Soc.* **1997**, *119*, 7153−7154. (b) Kobayashi, S.; Ishitani, H.; Ueno, M. *J. Am. Chem. Soc.* **1998**, *120*, 431−432. (c) Ishitani, H.; Ueno, M.; Kobayashi, S. *J. Am. Chem. Soc.* **2000**, *122*, 8180−8186. (d) Kobayashi, S.; Hamada, T.; Manabe, K. *J. Am. Chem. Soc.* **2002**, *124*, 5640−5641. (e) Kobayashi, S.; Matsubara, R.; Nakamura, Y.; Kitagawa, H.; Sugiura, M. *J. Am. Chem. Soc.* **2003**, *125*, 2507−2515. (f) Hagiwara, E.; Fujii, A.; Sodeoka, M. *J. Am. Chem. Soc.* **1998**, *120*, 2474−2475. (g) Fujii, A.; Hagiwara, E.; Sodeoka, M. *J. Am. Chem. Soc.* **1999**, *121*, 5450−5458. (h) Xue, S.; Yu, S.; Deng, Y.; Wulff, W. D. *Angew. Chem., Int. Ed.* **2001**, *41*, 2271−2274. (i) Trost, B. M.; Terrell, L. R. *J. Am. Chem. Soc.* **2003**, *125*, 338−339. (j) Juhl, K.; Gathergood, N.; Jørgensen, K. A. *Angew. Chem., Int. Ed.* **2001**, *40*, 2995−2997. (k) Ferraris, D.; Young, B.; Dudding, T.; Lectka, T. *J. Am. Chem. Soc.* **1998**, *120*, 4548−4549. (l) Ferraris, D.; Dudding, T.; Young, B.; Drury, W. J., III; Lectka, T. *J. Org. Chem.* **1999**, *64*, 2168−2169. (m) Taggi, A. E.; Hafez, A. M.; Lectka, T. *Acc. Chem. Res.* **2003**, *36*, 10−19. (n) Matsunaga, S.; Kumagai, N.; Harada, S.; Shibasaki, M. *J. Am. Chem. Soc.* **2003**, *125*, 4712−4713. (o) Harada, S.; Handa, S.; Matsunaga, S.; Shibasaki, M. *Angew. Chem., Int. Ed.* **2005**, *44*, 4365−4368. (p) Marques, M. M. B. *Angew. Chem., Int. Ed.* **2006**, *45*, 348−352. (q) For a review on catalytic asymmetric Mannich-type reaction, see: Kobayashi, S.; Ueno, M. In *Comprehensive Asymmetric Catalysis*; Jacobsen, E. N., Pfaltz, A., Yamamoto, H., Eds.; Supplement 1; Springer: Berlin, 2003; Chapter 29.5, p 143.
(14) For a review on (*S*)-proline-catalyzed Mannich reactions, see; Cordova, A. *Acc. Chem. Res.* **2004**, *37*, 102−112. See also, Marques, M. M. B. *Angew. Chem., Int. Ed.* **2006**, *45*, 348−352.
(15) Akiyama, T.; Takaya, J.; Kagoshima, H. *Synlett* **1999**, 1045−1048.
(16) (a) Akiyama, T.; Takaya, J.; Kagoshima, H. *Synlett* **1999**, 1426−1428. (b) Akiyama, T.; Takaya, J.; Kagoshima, H. *Tetrahedron Lett.* **2001**, *42*, 4025−4028. (c) Akiyama, T.; Takaya, J.; Kagoshima, H. *Adv. Synth. Catal.* **2002**, *344*, 338−347. Please see: (d) Manabe, K.; Mori, Y.; Kobayashi, S. *Synlett* **1999**, 1401−1402. (e) Manabe, K.; Mori, Y.; Kobayashi, S. *Tetrahedron* **2001**, *57*, 2537−2544. (f) Manabe, K.; Kobayashi, S. *Org. Lett.* **1999**, *1*, 1965−1967.
(17) Akiyama, T.; Takaya, J.; Kagoshima, H. *Tetrahedron Lett.* **1999**, *40*, 7831−7834.
(18) Quin, L. D. *A Guide to Organophosphorus Chemistry*; John Wiley & Sons: New York, 2000; Chapter 5, pp 133−165.
(19) Sudakova, T. N.; Krasnoshchekov, V. V. *Zh. Neorg. Khim.* **1978**, *23*, 1506−1508.
(20) Please see Scheme 4 in the Supporting Information for details.

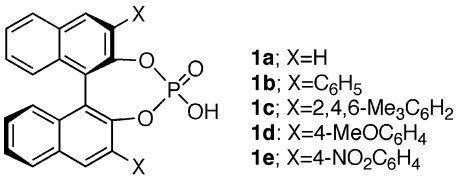

1

Figure 2. Chiral phosphoric acids.

Table 1. Effect of 3,3'-Substituents of Phosphoric Acid **1**[a]

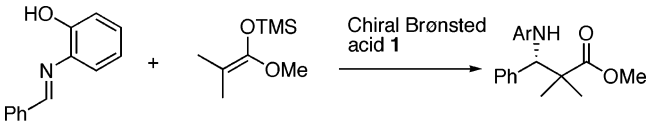

2a **3** **4a**

entry	Ar	time (h)	yield of **4a** (%)	ee (%)
1	H (**1a**)	22	57	0
2	Ph (**1b**)	20	100	27
3	2,4,6-$Me_3C_6H_2$ (**1c**)	27	100	60
4	4-$MeOC_6H_4$ (**1d**)	48	36	32
5	4-$NO_2C_6H_4$ (**1e**)	4	96	87

[a] Conditions: **2a** (1.0 equiv), **3** (3.0 equiv), **1** (30 mol %), toluene, −78 °C.

The catalysts **1** were readily prepared starting from (*R*)-BINOL[20] (Figure 2). Introduction of aryl groups onto the 3,3′-position was successfully achieved by the Suzuki−Miyaura coupling reaction. Bis-boronic acid[21] was used as a key intermediate for the preparation of 3,3′-substituted phosphoric acids **1**. The acid **1a** has been already utilized as a chiral resolving agent,[22] and its lanthanide salt was employed as a chiral catalyst,[23] but **1** itself had not been employed as a chiral catalyst as far as we know.

Results and Discussion

At the outset, a Mannich-type reaction of an aldimine **2a** and a ketene silyl acetal **3** was examined as a model reaction. On treatment of **2a** with **3** (3.0 equiv) in the presence of **1a** (0.3 equiv) in toluene at −78 °C, the Mannich-type reaction took place smoothly to give **4a** in a good yield as a racemic compound (Table 1, entry 1), which was determined by HPLC analysis with a chiral stationary phase column. Next we employed chiral phosphoric acids bearing aryl substituents on the 3,3′-positions **1b**−**1e**. Introduction of aromatic groups onto the 3,3′-position exerted a beneficial effect on the enantioselectivity. Use of **1b** as a chiral Brønsted acid increased the enantiofacial selectivity to 27% ee in toluene (entry 2). It is noted that 4-nitrophenyl groups on the 3,3′-position exhibits dual effects: (1) improvement of the enantioselectivity to 87%, (2) acceleration of the reaction rate, thereby completing the reaction in 4 h (entry 5). The absolute stereochemistry of **4a** was determined by comparison of the retention time of the chiral HPLC analysis of **4a** with that of the literature.[13h]

Further optimization of the reaction conditions elucidated that use of aromatic solvent exhibited high enantioselectivities, whereas protic solvent gave racemates (EtC_6H_e 83% ee; Et_2O, 30% ee; CH_2Cl_2, 13% ee; EtOH, 0% ee. A range of aromatic aldimines were found to be good substrates for the Mannich-type reaction catalyzed by 10 mol % of a chiral Brønsted acid **1e**.[24] Aldimines derived from aromatic and heteroaromatic aldehydes afforded adducts with good to high enantioselectivities. It is noted that the chemical yields were excellent in all the cases examined (see Table 4 in Supporting Information). Use of ketene silyl acetals bearing substituents on vinyl carbon gave high *syn* selectivity as well as excellent enantioselectivity (Scheme 2). A ketene silyl acetal derived from a propionate furnished the corresponding ester in 96% ee. Ketene silyl acetals derived from an α-oxy acetate also exhibited excellent *syn* selectivity and high enantioselectivity (see Table 5 in Supporting Information).

Furthermore, the present Mannich-type reaction can be achieved effectively even on a gram scale. Thus, on treatment of **2a** (1.06 g) with **3** in the presence of 10 mol % of **1e**, Mannich adduct **4a** was obtained in a quantitative yield with 87% ee without decreasing the enantioselectivity (Scheme 3). The

Scheme 2. Diastereoselective Mannich-Type Reaction

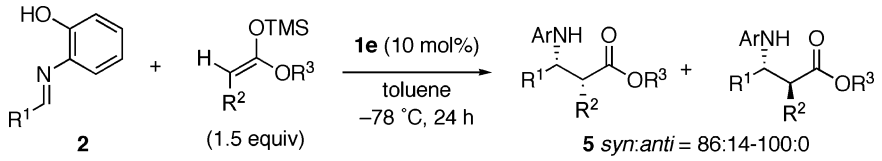

2 (1.5 equiv) **5** *syn*:*anti* = 86:14-100:0

85-96% ee

Scheme 3. Gram-Scale Synthesis of a β-Amino Ester

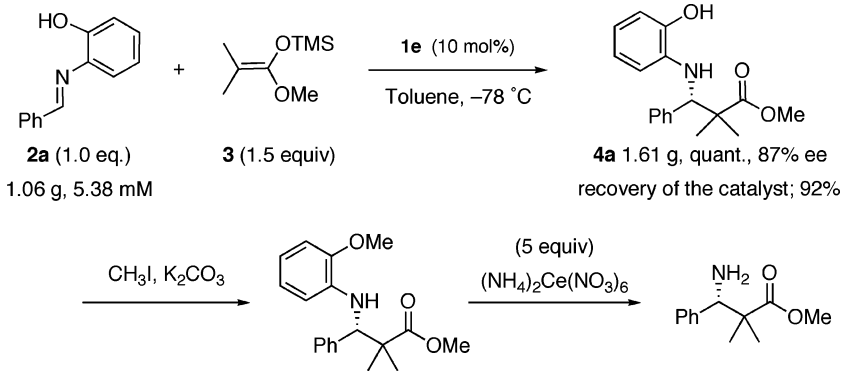

2a (1.0 eq.) **3** (1.5 equiv) **4a** 1.61 g, quant., 87% ee

1.06 g, 5.38 mM recovery of the catalyst; 92%

Table 2. Effect of the *N*-Aryl Group

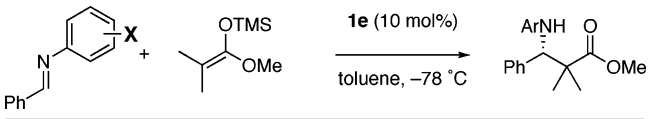

entry	X	time (h)	yield (%)	ee (%)
1	2-OH	13	98	89
2	4-OH	33	28	20
3	2-OCH_3	46	56	3
4	H	43	76	39

N-protecting group can be removed readily to furnish free amino acid ester in 47% yield from **4a**.

An interesting effect of the *N*-aryl group of aldimine was found in the present Mannich-type reaction. The 2-hydroxyphenyl group on nitrogen exhibited remarkably superior enantioselectivity compared to the 4-hydroxyphenyl group (Table 2, entry 1 vs 2). Because the enantioselectivity was lowered to 39% ee and 3% ee in the case of X = H and 2-OCH_3, the presence of the 2-hydroxy moiety of aldimine is essential to afford high yield and enantioselectivity (entry 1 vs 3, 4).

These results indicate that hydrogen bonding of the 2-hydroxy group on the *N*-aryl group plays an important role in combination with phosphoric acid activation to significantly amplify reactivity as well as enantioselectivity.

Investigation of the Reaction Mechanism: DFT Study. The intriguing effect of the *N*-aryl group of aldimine motivated us to study the reaction mechanism in detail. The 2-hydroxy group would form hydrogen bonding with phosphoryl oxygen to generate a nine-membered cyclic transition state we have previously proposed.[6b−e] However, the dual role of the Brønsted acid and hydrogen bond in the present reaction was still unclear. In combination with these experimental investigations, the mechanism of the present Mannich-type reaction was theoretically studied.[25] All calculations were performed with the Gaussian 98 package.[26] Geometries were fully optimized and characterized by frequency calculation using hybrid density functional theory (BHandHLYP) with the 6-31G*.[27] Free energies (298.15 K, 1 atm) and natural charges from the natural population analysis were also computed for the gas phase. In the continuum solvation model, the single-point energy calculations with the self-consistent reaction field (SCRF) calculation based on the polarizable continuum model (PCM,[28] $\epsilon = 2.379$ for toluene) were carried out at the same level as the one used for geometry optimization.

Two possible pathways (path 1, dicoordination pathway; path 2, monocoordination pathway) of the present reaction are shown in Scheme 4. The issue of which pathway proceeds favorably should be evaluated first, and hence we compared path 1 with path 2 to clarify the reaction mechanism in detail. Therefore, biphenolate (BIPOLate) was initially used instead of 3,3′-substituted BINOLate as a chemical model to reduce the computational cost. The issue of the *re*-facial selectivity in the present reaction is also addressed. As is known experimentally, only the 4-nitrophenyl group results in acceleration of the reaction rate keeping high enantioselectivity. We employed finally the 3,3′-substituted BIPOLate model bearing the 4-nitrophenyl group to clarify the origin of the preferential *re*-face attack.

Scheme 4. Mechanism of the Mannich-Type Reaction

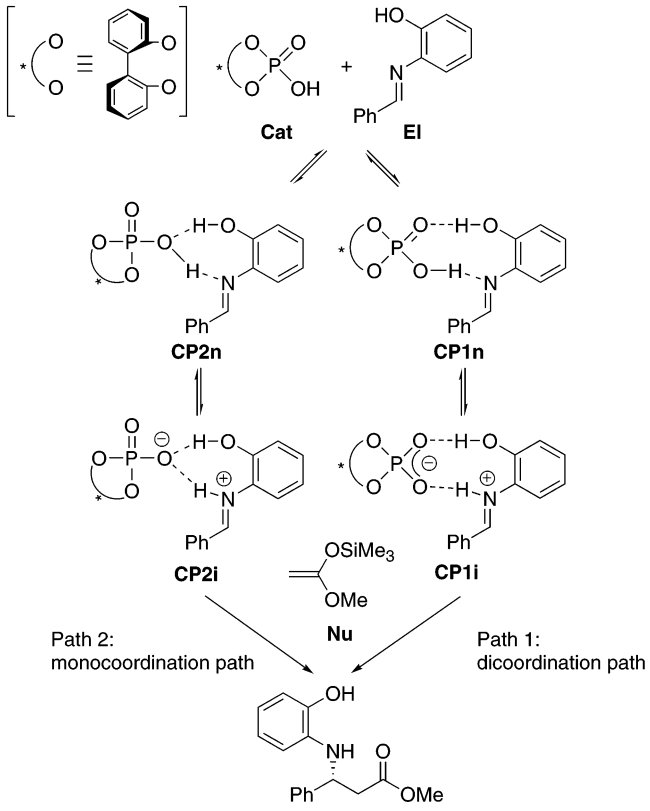

In both path 1 and path 2, there are two possible models of activation of aldimine (**El**): protonation and hydrogen-bonding

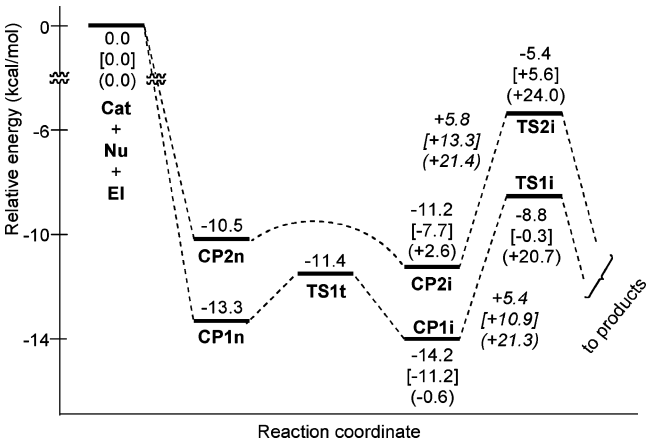

Figure 3. Energy profiles of dicoordination pathway (path 1) and monocoordination pathway (path 2). The potential energy of the sum of **Cat**, **Nu**, and **El** is set to zero. Activation energies are shown in italics, in parentheses are the free energies, and in brackets are the results of single-point energy calculations with the SCRF method based on PCM ($\epsilon = 2.379$ for toluene).

(21) Wipf, P.; Jung, J.-K. *J. Org. Chem.* **2000**, *65*, 6319−6337.
(22) Wilen, S. H.; Qi, J. Z. *J. Org. Chem.* **1991**, *56*, 487−489.
(23) For enantioselective synthesis using metal salt of BINOL phosphates, see: (a) Inanaga, J.; Sugimoto, Y.; Hanamoto, T. *New J. Chem.* **1995**, *19*, 707−712. (b) Furuno, H.; Hanamoto, T.; Sugimoto, Y.; Inanaga, J. *Org. Lett.* **2000**, *2*, 49−52.
(24) For details, please see Table 4 in the Supporting Information.
(25) After our submission of the manuscript, a report on the mechanistic and computational study on the phosphoric acid catalysis has been published. See: Gridnev, I. D.; Kouchi, M.; Sorimachi, K.; Terada, M. *Tetrahedron Lett.* **2007**, *48*, 497−500.
(26) Frisch, M. J. et al. *Gaussian 98*, revision A.11.4.; Gaussian, Inc.: Pittsburgh, PA, 2002.
(27) Hehre, W. J.; Radom, L.; Schleyer, P. v. R.; Pople, J. A. *Ab initio Molecular Orbital Theory*; John Wiley: New York, 1986 and references cited therein.
(28) Miertus, S.; Scrocco, E.; Tomasi, J. *Chem. Phys.* **1981**, *55*, 117−129.

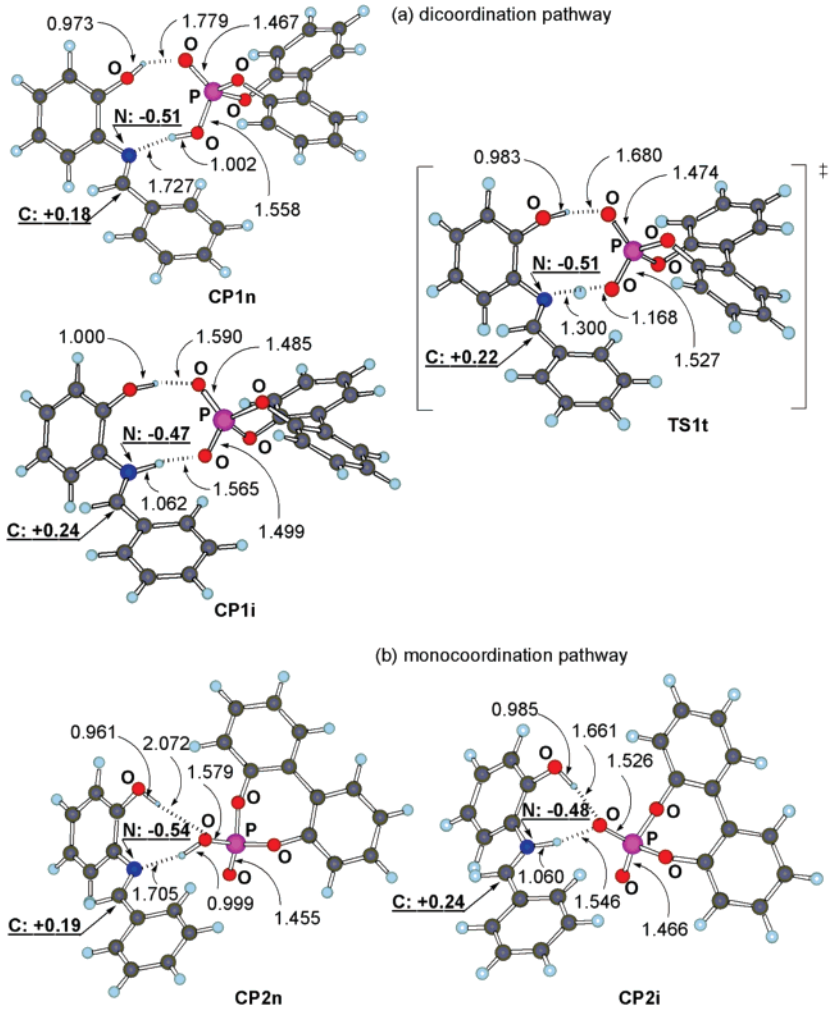

Figure 4. 3D structures of CPs and **TS1t** in (a) path 1 and (b) path 2 at the BHandHLYP/6-31G* level. Bond lengths are in Å, and natural charges are underlined and bold.

models. Protonation of aldimine generates a zwitterionic complex of iminium salt (**CP1i** or **CP2i**) followed by nucleophilic attack of ketene silyl acetal (**Nu**). In activation by hydrogen bonding, proton abstraction proceeds after the C−C bond formation on **CP1n** or **CP2n**. We explored the transition state (**TS**) of the C−C bond formation for two activation models. As a result, zwitterionic transition structures (**TS1i** and **TS2i**) were only found. In the hydrogen-bonding model, a proton spontaneously transferred from phosphoric acid (**Cat**) to the aldimine nitrogen in optimization of the **TS**. The present Mannich-type reaction, therefore, would proceed predominantly through protonation followed by nucleophilic attack via zwitterionic **TS**. The feasibility of the dicoordination (path 1) and monocoordination (path 2) pathways depending on the hydrogen-bonding mode on the phosphoryl oxygen is evaluated (Scheme 4). The relative energies in path 1 and path 2 were shown in Figure 3.

The zwitterionic complexes (**CP1i** and **CP2i**) generated by protonation and the hydrogen-bonding complex (**CP1n** and **CP2n**) are very close to each other in energy (within 1 kcal/mol). In a stationary point having a large number of low-frequency vibrational modes, the entropy contribution from the partition function for a low-frequency mode tends to be overestimated in a free energy calculation.[29,30] Such an entropic error would be problematic particularly in the protonation step of a very flat potential energy surface of our large molecular models having many low-frequency modes. Therefore, the relative energies of the zwitterionic **CPi** and **TSi** are only obtained from the free energies. As shown in path 1, the activation energy of protonation (**TS1t**) is only 1.9 kcal/mol and the proton-transfer reaction exhibits a very flat energy profile. This is reasonably applicable to path 2, and hence the protonation **TS** of **CP2n** was ignored in this calculation. In both path 1 and path 2, nucleophilic attack of ketene silyl acetal (**Nu**) to **CPi** yields the product via zwitterionic **TSi** with a moderate activation barrier, *ca.* 6 kcal/mol (*ca.* 21 kcal/mol in free energy). **TS1i** of a nine-membered cyclic transition state in path 1 is found to be lower in energy than **TS2i** in path 2 by 3.4 kcal/mol (3.3 kcal/mol in free energy). The relative stability of these complexes and transition structures retains in the solvation model (brackets in Figure 3).

Figures 4 and 5 show the 3D pictures of important stationary points. At the stage of protonation of **CP1n**, the structural feature other than the two-point hydrogen-bonding moiety is almost retained. The lengths of O−H, N−H, and P−O are changed dramatically through protonation. **CP1i** is regarded as the iminium phosphate due to the almost same two P−O bonds

(29) Ayala, P. Y.; Schlegel, H. B. *J. Chem. Phys.* **1998**, *108*, 2314−2325.
(30) See, for example: (a) Hamza, A.; Schubert, G.; Soós, T.; Pápai, I. *J. Am. Chem. Soc.* **2006**, *128*, 13151−13160.

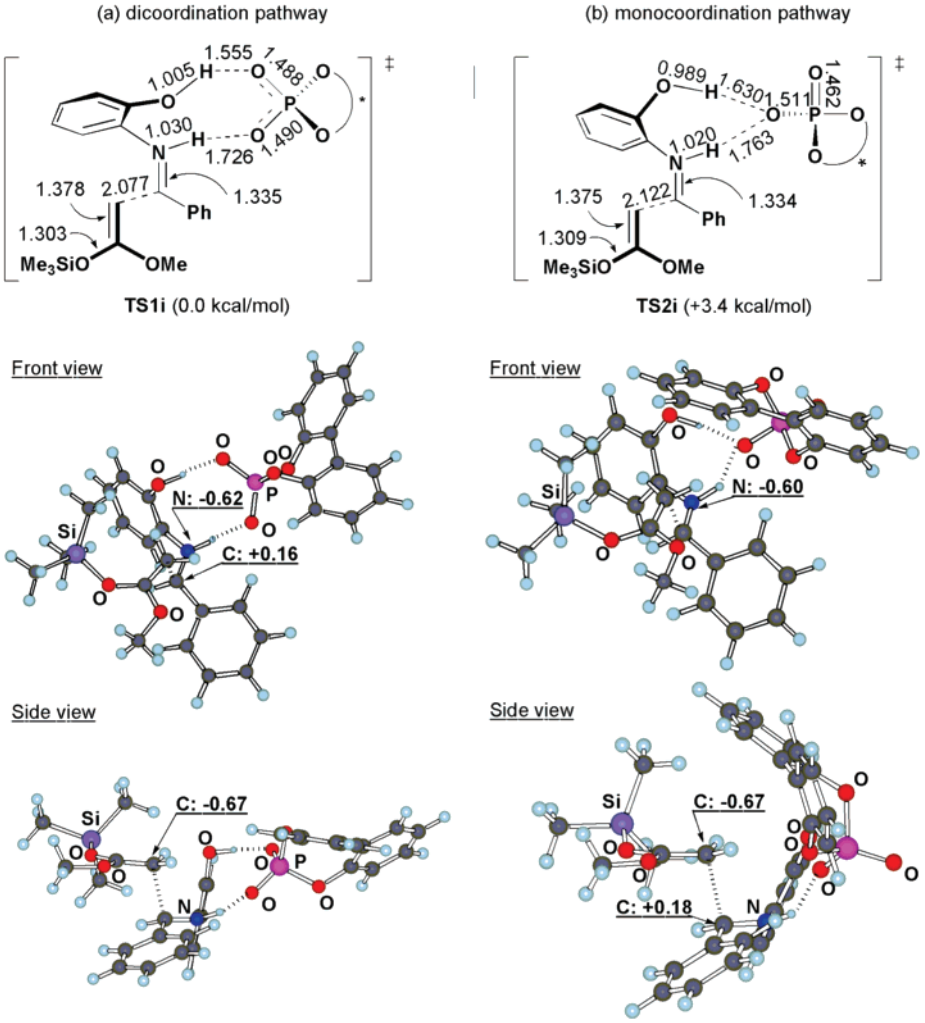

Figure 5. 3D structures of TSs in (a) path 1, **TS1i** and (b) path 2, **TS2i** at the BHandHLYP/6-31G* level. Bond lengths are in Å, and natural charges are underlined and bold.

Scheme 5. Possible Reaction Mechanism of the Present Mannich-Type Reaction

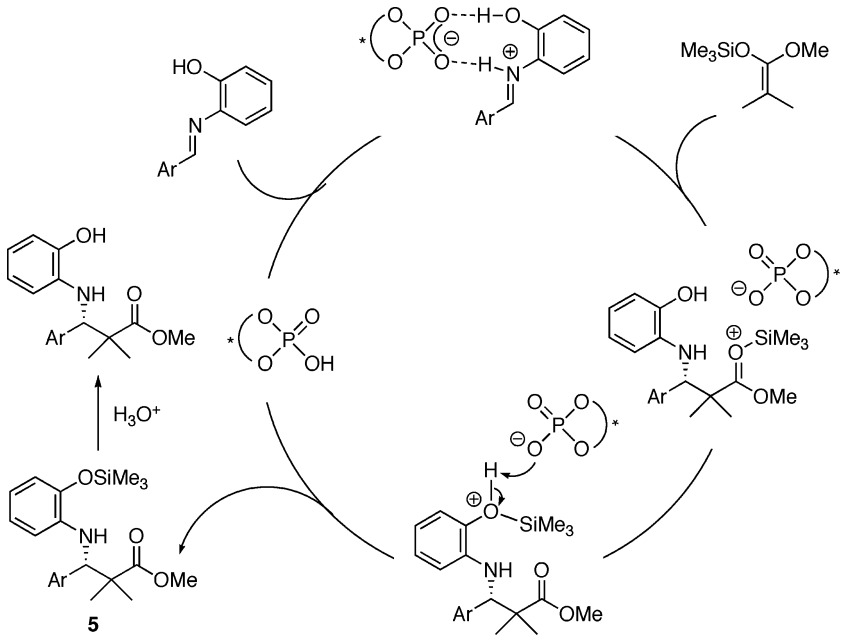

(e.g., phosphate anion) in comparison with **CP1n**. Natural population analysis showed that aldimine is more electrophilic in **CP1i** (natural charge on electrophilic carbon atom: + 0.24) than in **CP1n** (+0.18) in spite of similar gross structures of

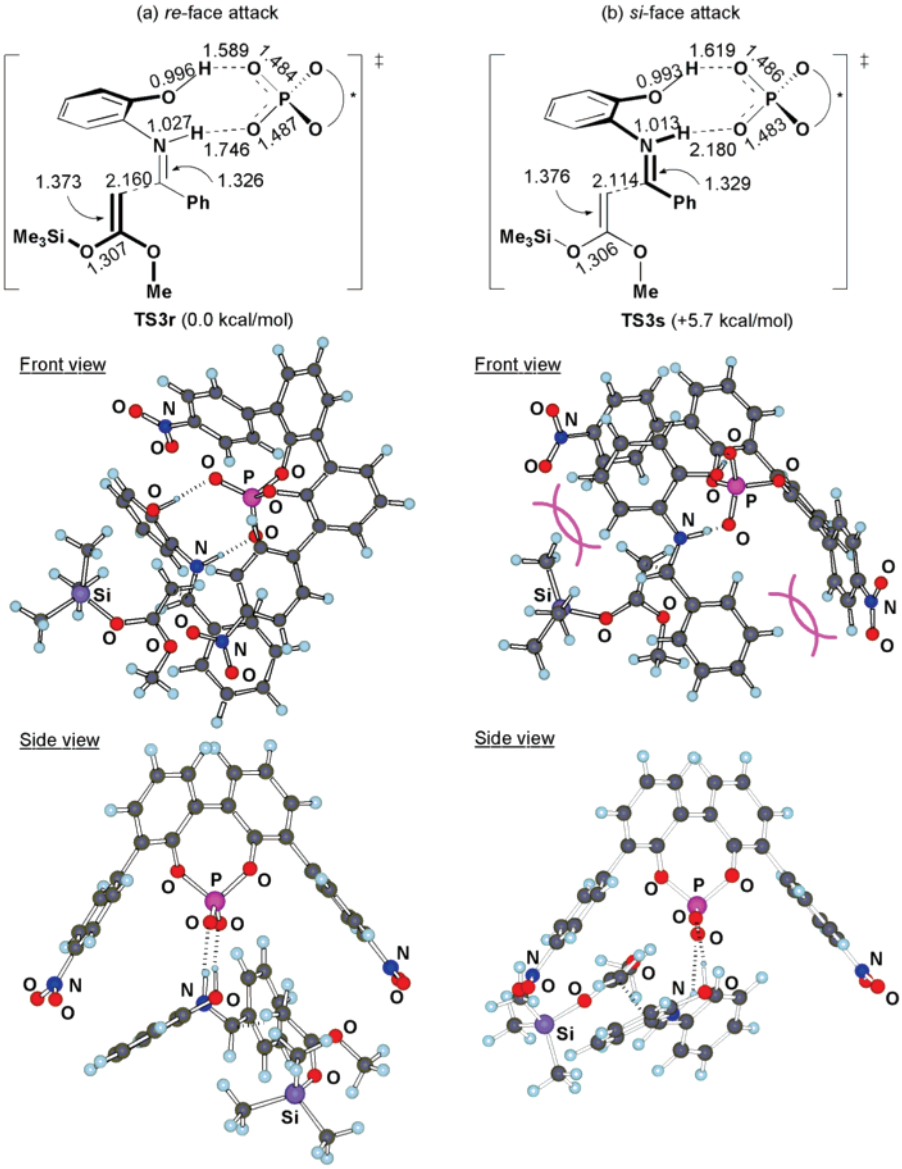

Figure 6. 3D structures of TSs in (a) *re*-face attack, **TS3r** and (b) *si*-face attack, **TS3s** at the BHandHLYP/6-31G* level. Bond lengths are in Å.

CP1i and **CP1n**. In **TS1t**, the proton stands around the center between the imine nitrogen atom and phosphoryl oxygen atom (Figure 4a). These structural and electron population features are also observed in **CP2n** and **CP2i** on path 2 (Figure 4b). The zwitterionic transition structures consist of iminium phosphate and ketene silyl acetal to afford highly complicated structures. The (*R*)-BIPOL moieties in **TS1i** and **TS2i** are located parallel and perpendicular to a C═N direction of aldimine, respectively. **TS2i** appears to be a more crowded concave structure for the attacking nucleophile than **TS1i**. In fact, the forming C−C bond of **TS2i** is longer than that of **TS1i** (**TS1i**, 2.077 Å; **TS2i**, 2.122 Å) (Figure 5).

To further study the origin of the energy difference (ΔE) between **TS1i** and **TS2i** (3.4 kcal/mol), which is very similar to that between **CP1i** and **CP2i** (3.0 kcal/mol), a fragment energy analysis was carried out (Table 3). **TS1i** and **TS2i** were divided into two fragments with a fixed geometry at the corresponding stationary points. The phosphoryl iminium salt fragment (**Fa**) and the ketene silyl acetal fragment (**Fb**) were

Table 3. Differences of Deformation (DEF) and Interaction (INT) Energies (kcal/mol) between **TS1i** and **TS2i**

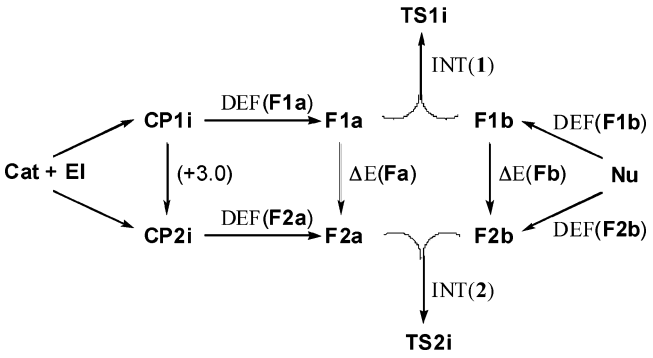

	CPi	TSi	DEF(Fa)	DEF(Fb)	INT
E(path 1)			+17.2	+7.1	−18.9
E(path 2)			+17.3	+5.9	−17.4
E(path 2) − E(path 1)	+3.0	+3.4	+0.1	−1.2	+1.5

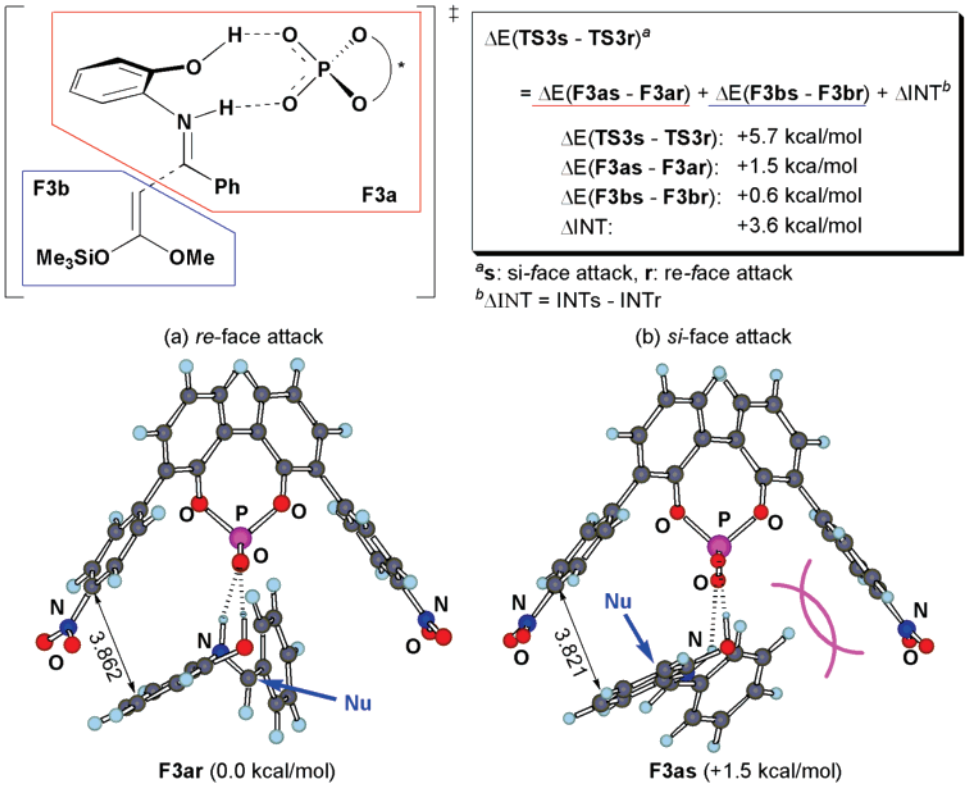

Figure 7. Differences of the iminium phosphate fragment (**F3a**) energy, the ketene silyl acetal fragment (**F3b**) energy, and interaction energy (INT) between **TS3r** and **TS3s**. The 3D structures of **F3a** in (a) *re*-face attack, **F3ar** and (b) *si*-face attack, **F3as** at the optimized structure by BHandHLYP/6-31G* calculation. Bond lengths are in Å.

deformed from the optimized original geometries of **CPi** and **Nu** to interact readily in **TSi**. The deformation energies of the iminium phosphate fragment, DEF(**Fa**), were same in both **TS1i** and **TS2i** (DEF(**F1a**), +17.2 kcal/mol; DEF(**F2a**), +17.3 kcal/mol). The ΔE between **F1a** and **F2a** (ΔE(**Fa**) in Table 3), therefore, corresponded to that between **CP1i** and **CP2i**. On the other hand, **TS1i** showed larger deformation energies for the **Nu** fragment, DEF(**Fb**), than those for **TS2i** (DEF(**F1b**), +7.1 kcal/mol; DEF(**F2b**), +5.9 kcal/mol). The interaction energy (INT) between **Fa** and **Fb** was calculated by the following equation.

$$\mathrm{INT} = (\text{total electronic energy of } \mathbf{TSi}) - \{\mathrm{DEF}(\mathbf{Fa}) + \mathrm{DEF}(\mathbf{Fb})\}$$

INT is larger in **TS1i** (−18.9 kcal/mol) than in **TS2i** (−17.4 kcal/mol). The stronger interaction of **F1** and **F2** in **TS1i** can be traced back to the shorter bond length of the forming C−C bond (**TS1i**, 2.077 Å; **TS2i**, 2.122 Å). Therefore, **Nu** in **TS1i** was more deformed than that in **TS2i** as described above. These results indicate that DEF(**Fb**) and INT essentially compensate each other. The ΔE between **TS1i** and **TS2i** originates mostly from that between **CP1i** and **CP2i**. The fragment energy analysis revealed that the energy difference between **TS1i** and **TS2i** is caused by the thermodynamic energy difference between **CP1i** and **CP2i** based on the hydrogen-bonding mode connecting the phosphoryl oxygen. In the dicoordination pathway (path 1), the iminium moiety tightly two-point coordinates to the phosphoryl oxygen throughout the reaction. It is overwhelmingly favored over the monocoordination pathway (path 2). In combination with the unique and important character of the 2-hydroxy group on the *N*-aryl group of aldimine experimentally observed, this computational analysis suggests the possible reaction mechanism as shown in Scheme 5. Indeed, *O*-trimethylsilyl ether **5** was observed as a major product in the crude mixture.

To explore the issue of the enantioselectivity in the present Mannich-type reaction, the 3,3′-substituted BIPOLate model was employed for the dicoordination pathway (path 1). Since introduction of the 4-nitrophenyl group on the 3,3′-positions is essential for the high enantioselectivity via *re*-face attack, the zwitterionic transition states of *re*-face (**r**) and *si*-face (**s**) attack were compared in the 3,3′-substituted BIPOLate model bearing the 4-nitrophenyl group. Structural and energetic characters of *re*-face (**TS3r**) and *si*-face (**TS3s**) attack of **Nu** were presented in Figures 6 and 7. The *re*-face attack is 5.7 kcal/mol more favored than *si*-face attack in agreement with the experimental result. It is noted that the *N*-aryl group of **El** and the 4-nitrophenyl group of **Cat** were forced to stack and formed a slipped-parallel structure by the aromatic stacking interaction.[31] This stacking interaction is predicted to fix the geometry of **El** in addition to the electrostatic interaction between the iminium cation and phosphoryl anion. The instability of **TS3s** would be attributed to the steric hindrance (purple curved lines) between the 4-nitrophenyl group of **Cat** and the $SiMe_3$ group of **Nu** (left side in Figure 6b) or the Ph group of **El** (right side in Figure 6b). These structural properties of **TS3r** and **TS3s** allowed us to examine in detail the origin of instability of **TS3s**. The ΔE

(31) In general, the DFT methods are not enough to correctly evaluate dispersion interaction in the weakly bounded system such as π-stacking interaction. It has been recently reported, however, that a half-and-half functional reproduces geometries and energetics for a π-stacked system with reasonable accuracy. See: (a) Waller, M. P.; Robertazzi, A.; Platts, J. A.; Hibbs, D. E.; Williams, P. A. *J. Comput. Chem.* **2006**, *27*, 491−504. (b) Romero, C.; Fomina, L.; Fomine, S. *Int. J. Quantum Chem.* **2005**, *102*, 200−208. (c) Zhao, Y.; Truhlar, D. G. *J. Chem. Theory Comput.* **2007**, *3*, 289−300.

between **TS3r** and **TS3s** is distributed into the phosphoryl iminium salt fragment (**F3ar** and **F3as** shown in Figure 7) energy, the ketene silyl acetal fragment (**F3br** and **F3bs**) energy, and the interaction energy (INT) between two fragments. The box of Figure 7 presents the ΔE of **F3a**, **F3b**, and INT between the *re*-face and *si*-face attacking pathways. The 3D pictures of **F3ar** and **F3as** reveal the arrangement of the Ph group of **El** is dramatically changed depending on the attacking face of **El** in contrast to similar structures of the stacking interaction moiety (red box in Figure 7). The Ph group of **El** is aligned parallel to the 4-nitrophenyl group of **Cat** in **TS3r**, whereas it is perpendicular in **TS3s**. Thus, **F3as** is found to be 1.5 kcal/mol less favored than **F3ar** by steric repulsion between the Ph group of **El** and the 4-nitrophenyl group of **Cat**. Both **F3br** and **F3bs** lie very close in energy. Two fragments, **F3a** and **F3b**, interact with each other more readily in **TS3r** than in **TS3s** since **TS3r** has a larger interaction energy (INT) than **TS3s** by 3.6 kcal/mol. This indicates that **Nu** approaches with unfavorable orientation in **TS3s** due to repulsive interaction between the $SiMe_3$ group of **Nu** and the 4-nitrophenyl group of **Cat** as mentioned above (Figure 6b). Consequently, both electrostatic and aromatic stacking interactions have significant roles in the high enantioselectivity to fix the geometry of **El** with a favorable orientation and to minimize the sterically repulsive interaction between the 3,3′-substituents of **Cat** and approaching **Nu**. The magnitude of the stacking interaction is sensitive to the nature of the substituent on the aryl group.[31a,32] The 4-nitrophenyl group would interact more attractively with the *N*-aryl group of aldimine than the normal Ph group due to significant electrostatic contributions to the aromatic stacking interaction.[33] Thus, the high enantioselectivity obtained by introduction of the 4-nitrophenyl group on 3,3′-positions would be caused by an increase of the stacking interaction rather than by an increase of the acidity of the phosphate group.

In summary, *we have developed chiral Brønsted acid catalyzed enantioselective Mannich-type reactions of aldimines with silyl enolates for the first time, and β-amino esters were obtained with high to excellent enantioselectivities under metal-free conditions*. Theoretical study elucidated that the two-point hydrogen bonding interaction makes the dicoordination pathway overwhelmingly favored over the monocoordination pathway in the present Mannich-type reaction. We found that the reaction proceeds through the protonation followed by the nucleophilic attack via zwitterionic and nine-membered cyclic TS. The intriguing issue of the *re*-facial selectivity was also well-rationalized. The two-point hydrogen-bonding moiety and aromatic stacking interaction between the 4-nitrophenyl group and *N*-aryl group are significantly important to fix the geometry of aldimine on the zwitterionic TS. The *si*-facial attacking TS is structurally less favored than the *re*-facial alternative due to repulsive interaction of the 3,3′-aryl substituents. The present Brønsted acid catalyzed reaction is potentially extended to a variety of enantioselective nucleophilic addition reactions to carbon−nitrogen double bond. Further application to other enantioselective reactions is in progress.

Acknowledgment. This work was partially supported by a Grant-in Aid for Scientific Research on Priority Areas "Advanced Molecular Transformation of Carbon Resources" from the Ministry of Education, Science, Sports, Culture, and Technology, Japan. J.I. thanks the JSPS Research Fellowships for Young Scientists. Computational time from the Research Center for Computational Science, Okazaki National Research Institute is deeply acknowledged.

Supporting Information Available: Experimental procedure, spectral data, and data of single-crystal X-ray analysis (CIF) and details of computation (Cartesian coordinates and absolute electronic energies of stationary points). This material is available free of charge via the Internet at http://pubs.acs.org.

JA0684803

(32) (a) Meyer, E. A.; Castellano, R. K.; Diederich, F. *Angew. Chem., Int. Ed.* **2003**, *42*, 1210−1250. (b) Hunter, C. A.; Lawson, K. R.; Perkins, J.; Urch, C. J. *J. Chem. Soc., Perkin Trans. 2* **2001**, 651−669. (c) Cockroft, S. L.; Hunter, C. A.; Lawson, K. R.; Perkins, J.; Urch, C. J. *J. Am. Chem. Soc.* **2005**, *127*, 8594−8595. (d) Tsuzuki, S.; Uchimaru, T.; Mikami, M. *J. Phys. Chem. A* **2006**, *110*, 2027−2033. (e) Sinnokrot, M. O.; Sherrill, C. D. *J. Chem. Phys. A* **2003**, *107*, 8377−8379.

(33) The mesityl group (in **1c**) has a different role from that of the 4-nitrophenyl group for the *re*-facial selectivity. It would generate a significant steric effect increasing the repulsive interaction for the $SiMe_3$ group of Nu. We are going to study other substituted BIPOL models.